Appl. Phys. A 75, 331–336 (2002)
DOI: 10.1007/s003390201342

Applied Physics A
Materials Science & Processing

M. DOGTEROM✉
M.E. JANSON
C. FAIVRE-MOSKALENKO*
A. VAN DER HORST
J.W.J. KERSSEMAKERS
C. TĂNASE
B.M. MULDER

Force generation by polymerizing microtubules

FOM Institute for Atomic and Molecular Physics (AMOLF), Kruislaan 407, 1098 SJ Amsterdam, The Netherlands

Received: 15 January 2002/Accepted: 11 February 2002
Published online: 22 April 2002 • **© Springer-Verlag 2002**

ABSTRACT Polymerization ratchets formed by the assembly of actin filaments and microtubules are possibly the simplest realizations of biological thermal ratchets. A variety of experimental evidence exists that significant forces are generated by these processes, but quantitative studies lag far behind similar studies for molecular motors such as kinesin and myosin. Here we present a discussion of the theory of polymerization ratchets as well as experimental techniques used in our laboratory for the study of forces generated by single growing microtubules. Data obtained with these techniques provide us with valuable information that may eventually allow us to distinguish between different models for the growth of microtubules.

PACS 87.16.Ka; 87.15.Rn

1 Introduction

In biological systems, thermal energies are similar in magnitude to interaction energies between macromolecules and the quanta of energy available from the burning of fuel molecules such as ATP (adenosine tri-phosphate). Thermal fluctuations therefore have a profound effect on the structure and dynamics of proteins. It is tempting to speculate on the possibility that nature has found mechanisms to use the energy available from thermal fluctuations and bias it into unidirected motion or work using a ratchet mechanism. Brownian or thermal ratchet models have been proposed to explain the motion of molecular motors such as kinesin, myosin, the ATP rotary motor, and ion pumps, all described elsewhere in this volume. As a consequence of the second law of thermodynamics, an energy source has to be available in addition to thermal fluctuations in order for a ratchet mechanism to perform work. In the original thermal ratchet proposed by Feynman, this energy source was a thermal gradient [1]. In biological systems, however, temperature gradients cannot be maintained easily and energy in these systems is derived from chemical bonds (stored in molecules like ATP) or the noncovalent binding energy between proteins.

✉ E-mail: dogterom@amolf.nl
*_Present address:_ Centre de Recherche Paul Pascal, Avenue Albert Schweitzer, 33600 Pessac, France

2 The polymerization ratchet

A fairly straightforward version of a biological thermal ratchet is the polymerization ratchet formed by so-called cytoskeletal proteins that self-assemble into linear filaments (see Fig. 1) [2–4]. The free energy available from the addition of a protein to a growing filament is available for mechanical work provided a mechanism is present to convert one into the other. In Fig. 1a one imagines that assembly takes place in contact with a 'barrier' on which a load is applied. In the cell, this load may be the stiffness of a membrane or the (viscous) drag on an intracellular macroscopic object being pushed forward by the assembling filament. Insertion of new subunits takes place at the contact point between the growing filament and the barrier. In the absence of thermal fluctuations there is no space between these two objects and proteins are physically prevented from attaching to the filament (Fig. 1a, top). Thermal fluctuations (in the form of diffusion of the barrier) create transient gaps that allow for the insertion and assembly of new subunits (Fig. 1a, middle). After assembly of a new subunit, the barrier can no longer diffuse back to its original location and has thus been 'pushed' forward by the assembling filament against the applied load (Fig. 1a, bottom). There is also a probability that subunits detach, which in this picture is independent of the presence of the barrier. The amount of work performed per assembling subunit is equal to the product of the subunit size and the load, which has a maximum equal to the assembly free energy [5]. The maximum forces one may expect are in the several piconewton range, since binding energies are on the order of several $k_B T$ and proteins are a few nanometers in size (one $k_B T$ corresponds to 4.1 pN nm at room temperature).

In practice, biological polymerization ratchets are more complicated than suggested in Fig. 1. Actin filaments, for instance, consist of two assembling protofilaments instead of one and microtubules consist of 13 protofilaments forming a hollow tube [6]. Despite the fact that this complicates the modeling aspects of the polymerization ratchet, it does not change the fact that forces generated by assembling filaments are real, and that they compete with forces generated by molecular motors in cellular functioning. The quantitative study of these forces and the understanding of the underlying molecular mechanisms are therefore not only of interest for physicists interested in experimental manifestations of ther-

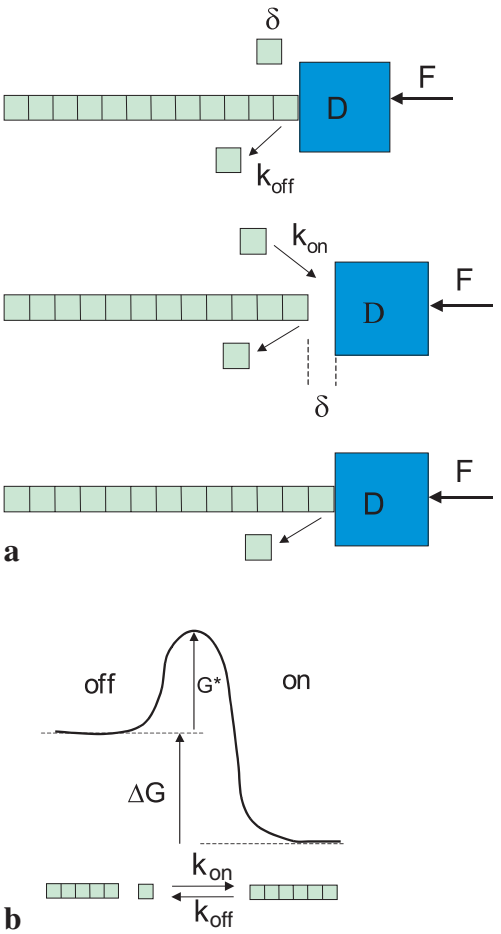

FIGURE 1 Force generation by linear filament assembly. **a** Schematic representation of the single-filament polymerization ratchet. A barrier (diffusion constant D) is pushed against a growing filament with force F (*top*). Thermal fluctuations occasionally create enough space to allow for the insertion of new subunits (size δ) at the contact point with rate k_{on} (*middle*), thereby effectively pushing the object forward (*bottom*). At all times subunits detach with rate k_{off}. **b** The free-energy difference ΔG between the off- and on-states of a subunit drives the polymerization reaction. The activation energy G^* affects the absolute value of the on- and off-rates, but not their ratio

mal ratchets, but are also important to biologists interested in the role and regulatory principles of forces involved in various forms of cellular motility.

In this paper we start by presenting the equations that describe the single-filament polymerization ratchet described above. After a brief introduction to the biology of cytoskeletal filaments, we then focus on experiments with single growing microtubules in vitro [7], and discuss the specific models available for this system [8–10].

3 The single-filament model

In the ratchet model described above, the rate at which new subunits manage to attach is in principle a function of the magnitude of the load, F, and the time scale of relevant positional fluctuations of the barrier (determined by the diffusion constant D of the barrier and the size δ of a protein subunit). When diffusion of the barrier over distances of order δ is fast compared to the time between subsequent subunit additions, the diffusion constant is no longer of importance [2]. The rate of assembly is then simply the (concentration-dependent) bare rate in the absence of any force or barrier, given by k_{on}, multiplied by the probability of opening a gap large enough for a new subunit to insert. This probability depends on the energy associated with moving the load F over a distance δ and is given by $\exp(-F\delta/k_{\mathrm{B}}T)$, where k_{B} is Boltzmann's constant and T is the absolute temperature. In this simplest case the velocity of polymerization in the presence of a load is given by

$$V(F) = \delta\left(k_{\mathrm{on}}\mathrm{e}^{-F\delta/k_{\mathrm{B}}T} - k_{\mathrm{off}}\right) , \tag{1}$$

where k_{off} is the rate of disassembly.

The stall force, which is defined as the force needed to bring the growth velocity to zero, is given by

$$F_{\mathrm{stall}} = \frac{k_{\mathrm{B}}T}{\delta}\ln\frac{k_{\mathrm{on}}}{k_{\mathrm{off}}} . \tag{2}$$

This last result can of course also be predicted from simple thermodynamic arguments [11]. Figure 1b shows schematically the free-energy difference ΔG between the on- and off-states of a subunit as well as the activation barrier G^* for transitions between the two. The absolute values of the on- and off-rates depend on the activation energy, but the ratio $k_{\mathrm{on}}/k_{\mathrm{off}}$ does not, and is simply given by $\exp(\Delta G/k_{\mathrm{B}}T)$. The amount of work per assembling subunit that is needed to balance the reaction is thus given by

$$F_{\mathrm{stall}}\delta = \Delta G = k_{\mathrm{B}}T\ln\frac{k_{\mathrm{on}}}{k_{\mathrm{off}}} . \tag{3}$$

These arguments also predict the ratio between the rates of assembly and disassembly at smaller forces. In the presence of force, the gain in free energy due to assembly of a subunit is reduced by the amount of work performed to $\Delta G' = \Delta G - F\delta$, which gives

$$\frac{k_{\mathrm{on}}}{k_{\mathrm{off}}}(F) = \mathrm{e}^{(\Delta G - F\delta)/k_{\mathrm{B}}T} = \frac{k_{\mathrm{on}}}{k_{\mathrm{off}}}(0)\mathrm{e}^{-F\delta/k_{\mathrm{B}}T} . \tag{4}$$

This formula gives no information about the absolute effect of force on the on- and off-rates (for this, additional information on the effect of force on the activation energy G^* is needed). The result is however consistent with the ratchet model (1), where it is implicitly assumed that the rate of disassembly is unaffected by the load. If no such assumptions are made, a more general form of the force–velocity curve predicted by thermodynamic arguments is given by

$$V(F) = \delta\left(k_{\mathrm{on}}\mathrm{e}^{-qF\delta/k_{\mathrm{B}}T} - k_{\mathrm{off}}\,\mathrm{e}^{(1-q)F\delta/k_{\mathrm{B}}T}\right) , \tag{5}$$

where the value of q depends on how much the off-rate is affected by the force relative to the on-rate.

4 Force generation by cytoskeletal filaments

The mechanical framework (cytoskeleton) of higher-order (eukaryotic) cells consists of three types of protein filaments: actin filaments, intermediate filaments, and microtubules [6]. The assembly or polymerization of both actin filaments and microtubules has been implicated in cellular

force generation processes. (Note that both these filaments are also known to serve as tracks for motor proteins, where they play a more passive role in the generation of force [12].) Examples are: the pushing forward of membranes by polymerizing actin filaments in the leading edge of crawling cells [13]; the propulsion of *Listeria* bacteria through their host cell, again by polymerization of actin filaments [14, 15]; and the motion of chromosomes by the assembly and disassembly of microtubules during the process of cell division [16]. Focusing on this last example, Fig. 2 shows a schematic view of the structure of an individual microtubule [17] as well as the arrangement of microtubules in contact with chromosomes in a dividing cell [18]. Individual microtubules consist of 13 protofilaments forming a hollow tube, assembled from tubulin protein dimers. Microtubules in the mitotic spindle are nucleated by two organelles called centrosomes that position on opposite sides of the chromosomes. These microtubules are by no means static structures. If one focuses on a single microtubule, one observes that periods of net assembly (at typical rates of several micrometers per minute) are randomly alternated by periods of somewhat faster net disassembly. The balance between k_{on} and k_{off} radically changes when a microtubule switches from net growth to net shrinkage (a catastrophe) or vice versa (a rescue). This process, termed dynamic instability, depends on the hydrolysis of associated GTP (energy) molecules (Fig. 2a), is crucial for the length control of the microtubules, and is heavily regulated by the cells' biochemical machinery [17]. The dynamic ends of microtubules attach to specialized regions of the chromosomes, called kinetochores [19], in such a way that assembly and disassembly continues to take place [20]. It is believed that during periods of net assembly and net disassembly both pushing and pulling forces are generated on the chromosomes [16].

Several in vitro experiments have demonstrated the force-generating capabilities of cytoskeletal filaments. Growing microtubules are able to deform artificial lipid bilayers [21, 22] and pull tubules from membranes in cell extracts [23]. Shrinking microtubules have been shown to generate force on objects attached to their end [24]. Although in vivo it is very difficult to distinguish the role of polymerization forces from contributions by motor proteins, growing microtubules in for example yeast cells have clearly been shown to be able to deform themselves [25]. Actin polymerization can drive the propulsion of *Listeria* bacteria and even protein-coated microspheres in cellular extracts as well as appropriate mixtures of purified components [14, 15]. In these systems dense meshworks ('comet tails') of actin filaments are formed that drive motility in a way similar to what has been proposed for the propulsion of the leading edge of crawling cells. Several models have been put forward to explain the forces generated by such a collection of assembling filaments, some of which are based on a ratchet mechanism [26–28].

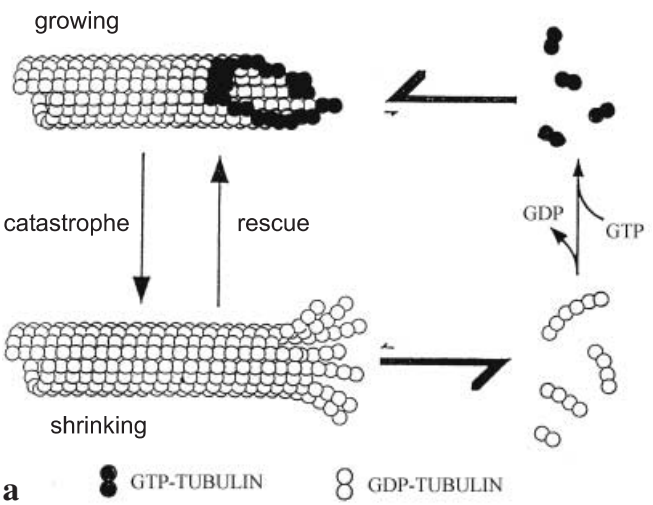

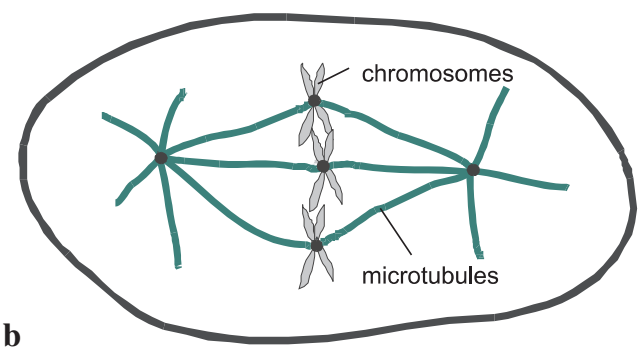

FIGURE 2 **a** Schematic representation of the structure and assembly dynamics of microtubules (adapted from [17]). Thirteen linear protofilaments built from tubulin protein dimers form a hollow tube of 25-nm diameter. Assembling tubulin subunits have a bound GTP molecule (guanosine triphosphate) that is hydrolyzed to GDP (guanosine di-phosphate) upon incorporation into the microtubule. When GDP-tubulin is exposed at the end, the microtubule switches to a state of rapid disassembly. The molecular details of this switch (termed a catastrophe) as well as the reverse process (a rescue) are still poorly understood. **b** Schematic representation of the mitotic spindle, emphasizing the connection between microtubule ends and chromosomes

5 Experiments on single microtubules

In our group we developed an experimental set-up using lithography techniques that allows us to study, quantitatively, the forces generated by single growing microtubules. Figure 3a shows schematically our set-up. Short pieces of stabilized microtubules are biochemically attached to a glass substrate. On this substrate, lines (15-μm wide, 2-μm high) of silicon monoxide are deposited that serve as barriers for growing microtubules. When tubulin proteins are added at sufficiently high temperature (15–35 °C) and concentration (a few mg/ml) [29], microtubules grow from the templates, some of which encounter the deposited barriers. An important technical detail of these barriers is that we create a small 'undercut' by briefly etching the substrates in HF. These undercuts force the microtubule ends to stay in the focal plane of the microscope and prevent them from sliding upwards after reaching the barrier.

When microtubules hit the barrier they generally continue to grow. To accommodate the increase in length two things can happen: either the elongating microtubule end slides laterally along the barrier, giving rise to a modest deflection of the microtubule, or the microtubule end is hindered in this lateral motion (by an encountered irregularity in the barrier profile), resulting in a more dramatic buckling of the microtubule with its growing end pivoting around a fixed contact

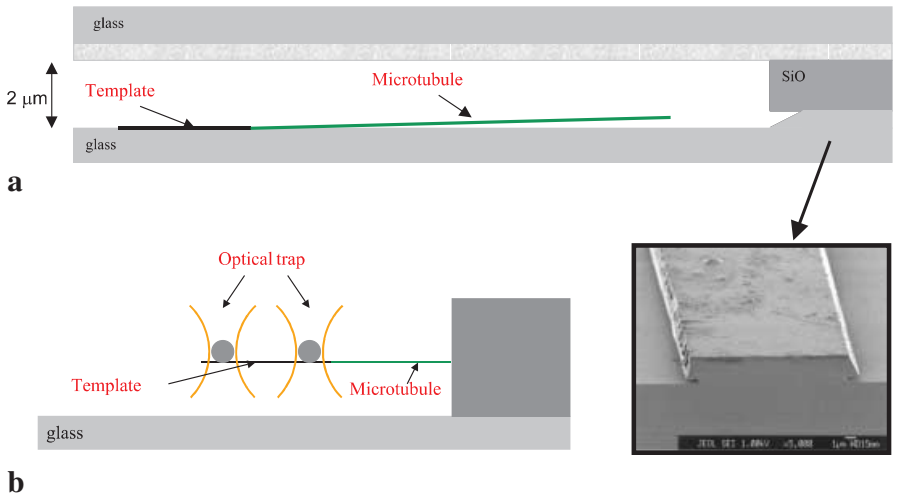

FIGURE 3 Schematic representation of two in vitro experimental set-ups that are used in our laboratory to study force generation by single growing microtubules. **a** A short piece of stabilized microtubule (template) is attached through a biotin–streptavidin linkage to the surface of a microscope coverslip. Barriers (2-μm high, 15-μm wide) of SiO are vapor-deposited on this coverslip and a small undercut is created using HF etching. The electron micrograph shows the profile of such a barrier. Microtubules that grow from the template hit the barrier and buckle as a consequence of the force generated by the assembly process (see Fig. 4a). **b** Alternatively, two micron-sized beads are attached to the template and held in two optical traps. The traps are used to orient the growth of the microtubule in the direction of a rigid barrier and to measure directly the force generated by the growth of the microtubule (see Fig. 4c)

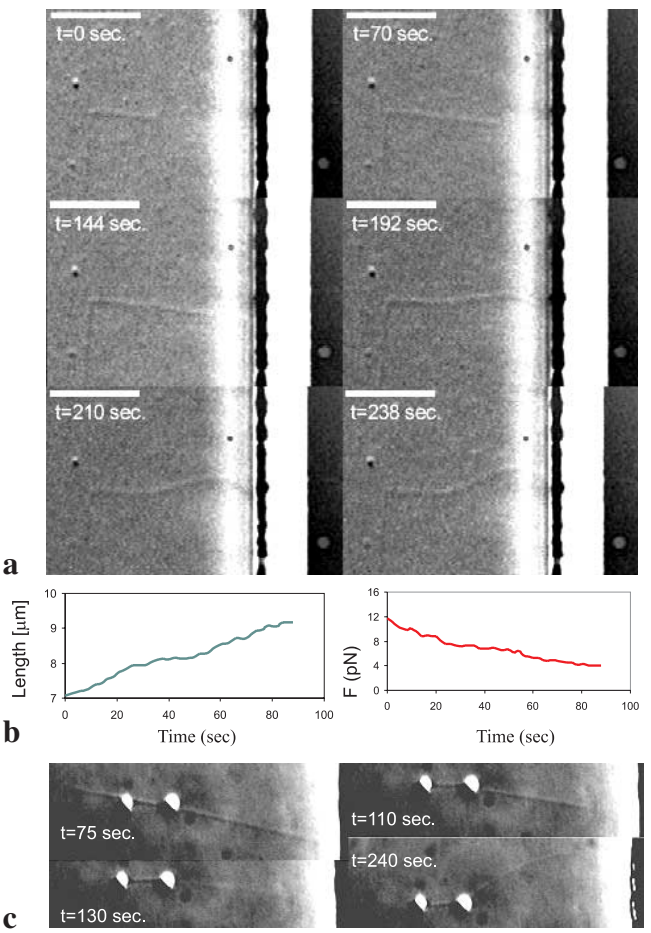

FIGURE 4 **a** Time sequence of a buckling microtubule as observed by video-enhanced DIC (Differential Interference Contrast) microscopy (see Fig. 3a) [35]. At time zero growth is initiated by a template. After reaching the barrier on the *right*, the microtubule continues to grow and buckles. *Bar* is 5 μm. **b** Analysis of the buckling shapes in **a** allows us to determine the force and the length of the microtubule as a function of time. Under the conditions used here a free microtubule grows at approximately 2.5 μm/min. **c** Preliminary results obtained with the trapping technique. A long microtubule held by two beads in two traps reaches the barrier, continues to grow, and buckles. Tracking of the position of the beads with nanometer resolution allows us to measure the force on the microtubule directly and to compare it to the force derived from the buckling shape. The distance between the barrier (on the *right*) and the closest bead is 14.5 μm

point with the barrier (see Fig. 4a). In this last case the elastic restoring force of the buckled microtubule puts a significant load on the growth of the microtubule, directly affecting the further growth of the filament. Using image analysis and fitting procedures, the shape of the growing microtubule can be related to both the magnitude and the direction of the force acting on the microtubule end, provided an independent measurement of the flexural rigidity is available [30]. At the same time the increase in microtubule length and thus the growth velocity can be derived from these fits (Fig. 4b).

Note that compared to the situation in Fig. 1, it is in this case not the barrier that is fluctuating but the position of the assembling filament end itself. In addition the load is not applied externally, but caused by the elastic deformation of the filament itself. This however does not change the ratchet behavior, as long as the fluctuations in the gap size are sufficiently fast and the applied load is not itself dependent on the gap size (an example of a gap-dependent force is given by the elastic Brownian ratchet discussed in [26]). Sufficiently fast in this context means that diffusion over nanometer distances should be faster than the assembly rate of a subunit (on the order of 50 s^{-1} for microtubules in vitro).

With this 'buckling' technique questions can be answered about the effect of force on the growth velocity of the microtubule [7], to be compared with force–velocity curves predicted by various growth models (see below). Also, the effect of force on the catastrophe frequency (the probability to switch from growing to shrinking) can be studied [31]. The parameter that cannot be measured directly is the stall force. Due to the geometry of the experiment the force on the microtubule end never increases after the buckling of the microtubule has started, and in fact decreases during the course of the experiment (due to the strong dependence of the critical buckling force on the filament length: $F_c \sim L^{-2}$ [30]). Microtubules that are attached relatively close to the barrier stop growing as soon as they encounter the barrier, apparently because the force needed to overcome their critical buckling force is too large. In these cases we have no direct way of measuring the force applied (although estimates can be made). As the stall force may turn out to be an important parameter in distinguishing between different growth models we designed a second experimental set-up based on optical

tweezers techniques (see Fig. 3b). In this set-up the microtubule template is attached to two micron-sized silica spheres. These beads are each held in an optical trap orienting the growth direction of the microtubule towards a barrier similar to the one used in the previous experiment. In this case the distance to the barrier should ideally be chosen such that the force needed to buckle the microtubule is larger than the expected stall force. In response to the growth of the microtubule the beads will move with respect to the centers of the optical traps, thereby linearly increasing the force on the growing microtubule end until growth stops. An independent calibration of the trap stiffness then gives a direct measure of the force applied [32]. Preliminary results of this experiment (with long, buckling microtubules, see Fig. 4c) indicate that forces acting on the beads are indeed consistent with the forces derived from the buckling shapes of the microtubules.

6 Ratchet models for growing microtubules

Fig. 5 shows the force–velocity data for microtubules published so far, obtained with the buckling technique. One should take care in comparing these experimental results with the simple Brownian ratchet model described above. Even though single growing microtubules provide in our opinion the simplest experimental model system so far (given the lack of experiments with individual actin filaments and the more complex structure of the actin comet tails produced by Listeria), they represent by no means the simplest possible example of a polymerization ratchet. This would consist of a single linear filament as sketched in Fig. 1a, whereas microtubules consist of 13 laterally connected protofilaments forming a hollow tube. The geometrical details of the growth process of microtubules are not well known. In addition, there is the possibility that the hydrolysis of GTP, responsible for the occasional switching to a shrinking state, should be taken into account to understand the response of the growth process to force. In this case the stall force may no longer be simply connected to the free energy associated with tubulin assembly.

Given what is known about the structure of microtubules, it is tempting to try to include the geometrical details of a growing microtubule into a thermal ratchet model. A simplistic generalization of the original ratchet model describing the growth process of a polymer consisting of two filaments (as is the case for actin) certainly did not fit the available data [2, 7]. In this case it was assumed that the size of the gap needed to insert each new subunit was equal to the added microtubule length per dimer: δ/n, where n is the number of filaments in the polymer. Mogilner and Oster therefore generalized the ratchet model described above in a different way [8]. They assumed 13 laterally connected, independently growing ratchets, initially arranged as a staircase with subsequent shifts equal to one-thirteenth of the subunit size, with the longest filament in contact with the barrier at any time. Growth of any particular filament requires a fluctuation of the barrier large enough for that filament to insert a new subunit, which thus becomes a function of the distance of the end of that filament to the barrier. Through numerical solutions as well as simulations of this model the steady-state distribution of filament–barrier distances can be determined as a function of applied force, and with this the average growth rate can be calculated. Even though this model makes a lot of implicit assumptions, the outcome fits the available experimental data very well. The fit is however very insensitive to the only free parameter in this model: the stall force (i.e. the ratio between the bare on- and off-rates, given that their difference is fixed by a measurement of the growth velocity at zero force), and no firm conclusions about the stall force can be made [9]. One can make reasonable variations to this model that fit the data equally well [33]. For example, the initial 'shift' between subsequent protofilament tips in a real microtubule is closer to one-eighth of a subunit. Also, it seems reasonable to assume at least some interaction between neighboring protofilaments. Even though there is no reason to insist on the details of these models, the outcome of the comparison with the experimental data might in fact suggest that the end of a growing microtubule looks more like a irregular pointed structure than a blunt end (under the current experimental conditions). Instead of making explicit assumptions about the geometrical details of the growth process, Kolomeisky and Fisher have suggested a different approach to analyzing the available data [10]. In a spirit similar to (5), a general form of the force–velocity relation based on thermodynamic considerations can be written down as:

$$V(F) = \frac{\delta}{n}\left(k_{\mathrm{on}} \mathrm{e}^{-qFd_1/k_{\mathrm{B}}T} - k_{\mathrm{off}}\,\mathrm{e}^{(1-q)Fd_1/k_{\mathrm{B}}T}\right), \qquad (6)$$

where $n = 13$ represents the number of protofilaments. Here four parameters are free to fit: the size of the force generating length increase d_1 (which for a multifilament polymer can be less than the subunit size), the bare (microtubule) on- and off-rates, and the distribution of the load dependence between the on- and off-rates. Of course, reasonable fits can be obtained. This expression still assumes that the on- and off-rates are related to each other through the gain in free energy of a simple addition of one subunit, and therefore does not take into account the possible role of GTP hydrolysis. Also, the parameters q and d_1 may in principle themselves be a function of the force (as is effectively the case for the Mogilner and Oster model for d_1), providing an even larger set of possible fitting parameters. Given enough experimental data this approach is

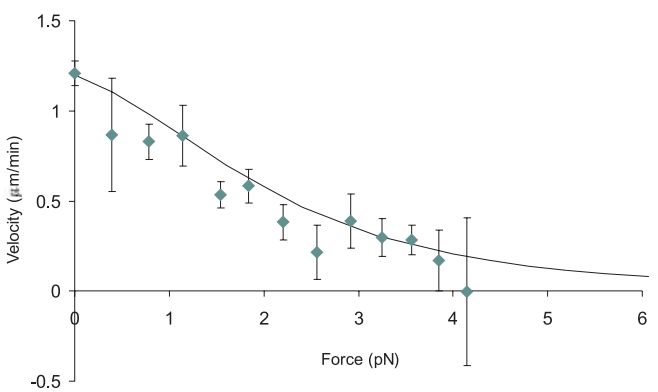

FIGURE 5 Force–velocity curve of microtubule growth derived from experiments similar to Fig. 4a [7]. The *solid line* indicates the result from a simulation of a ratchet model that assumes 13 independently growing parallel filaments [8]. This fit is relatively insensitive to the only free parameter in this model, the stall force (arbitrarily chosen to be 18.5 pN in this case) [9]

clearly the most general, but for the moment the number of free parameters seems too large to draw strong conclusions from fits obtained with (6).

7 Conclusions and perspectives

The experiments on single growing microtubules presented here provide us with a straightforward realization of a biological thermal ratchet. They have shown us that biologically significant forces (on the order of several piconewtons) can indeed be generated by the assembly of cytoskeletal filaments. Comparisons with simple thermal ratchet models should be taken with care, since the structure of a single growing microtubule is in fact quite complicated. (To make matters worse, electron-microscopy studies of microtubules have suggested that growing ends consist of sheet-like structures that close into hollow tubes during the assembly process [34].) Clearly, the available models that attempt to take this complexity into account provide many possibilities and additional data are desperately needed. New sets of data taken at higher initial growth velocities than presented in Fig. 5 (see for example Fig. 4) in fact appear to be inconsistent with the simplest independent 13-ratchet model [35]. Careful analysis of such multiple data sets should eventually teach us about the mechanism and geometrical details of the growth process. In addition, we hope that experiments using optical trapping techniques will provide us with complementary information, in particular on the stall force, narrowing down even further the available microscopic models. From a biological point of view, studying the forces generated in contact with an artificial glass barrier may not be all that interesting. What will be important in the future is to repeat these types of experiments with barriers consisting of chromosomes, kinetochore complexes, or simple motor-coated surfaces. Comparison with our current experiments may reveal important hints as to how molecular growth details and the force-generating process are affected or even regulated by interaction with these specific barriers.

ACKNOWLEDGEMENTS This work is part of the research program of the 'Stichting voor Fundamenteel Onderzoek der Materie (FOM)', which is financially supported by the 'Nederlandse organisatie voor Wetenschappelijk Onderzoek (NWO)'. We thank K. Visscher for valuable advice on the optical trapping technique, and F. Jülicher and many other colleagues for discussions on the polymerization ratchet. One of us (M.D.) would like to thank B. Yurke, with whom the first experimental data were obtained.

REFERENCES

1 R.P. Feynman, R.B. Leighton, M. Sands: *The Feynman Lectures on Physics* (Addison-Wesley, Reading, MA 1963)
2 C.S. Peskin, G.M. Odell, G.F. Oster: Biophys. J. **65**, 316 (1993)
3 L. Mahadevan, P. Matsudaira: Science **288**, 95 (2000)
4 J.A. Theriot: Traffic **1**, 19 (2000)
5 A. Parmeggiani, F. Julicher, A. Ajdari, J. Prost: Phys. Rev. E **60**, 2127 (1999)
6 B. Alberts, D. Bray, J. Lewis, M. Raff, K. Roberts, J.D. Watson: *Molecular Biology of the Cell* (Garland, New York, London 1994)
7 M. Dogterom, B. Yurke: Science **278**, 856 (1997)
8 A. Mogilner, G. Oster: Eur. Biophys. J. **28**, 235 (1999)
9 G.S. van Doorn, C. Tănase, B.M. Mulder, M. Dogterom: Eur. Biophys. J. **29**, 2 (2000)
10 A.B. Kolomeisky, M.E. Fisher: Biophys. J. **80**, 149 (2001)
11 T.L. Hill: *Linear Aggregation Theory in Cell Biology* (Springer, New York, Berlin, Heidelberg 1987)
12 R.D. Vale, R.A. Milligan: Science **288**, 88 (2000)
13 D. Bray: *Cell Movements: from Molecules to Motility* (Garland, New York 2000)
14 L.A. Cameron, P.A. Giardini, F.S. Soo, J.A. Theriot: Nat. Rev. Mol. Cell Biol. **1**, 110 (2000)
15 D. Pantaloni, C.L. Clainche, M.-F. Carlier: Science **292**, 1502 (2001)
16 S. Inoué, E.D. Salmon: Mol. Biol. Cell **6**, 1619 (1995)
17 A. Desai, T.J. Mitchison: Annu. Rev. Cell Dev. Biol. **13**, 83 (1997)
18 T. Wittmann, A. Hyman, A. Desai: Nat. Cell Biol. **3**, E28 (2001)
19 C.L. Rieder, E.D. Salmon: Trends Cell Biol. **8**, 310 (1998)
20 A.J. Hunt, J.R. McIntosh: Mol. Biol. Cell **9**, 2857(1998)
21 M. Elbaum, D.K. Fygenson, A. Libchaber: Phys. Rev. Lett. **76**, 4078 (1996)
22 D.K. Fygenson, J.F. Marko, A. Libchaber: Phys. Rev. Lett. **79**, 4497 (1997)
23 C.M. Waterman-Storer, J. Gregory, S.F. Parsons, E.D. Salmon: J. Cell Biol. **130**, 1161 (1995)
24 V.A. Lombillo, R.J. Stewart, J.R. McIntosh: Nature **373**, 161 (1995)
25 P.T. Tran, L. Marsh, V. Doye, S. Inoué, F. Chang: J. Cell Biol. **153**, 397 (2001)
26 A. Mogilner, S. Oster: Biophys. J. **71**, 3030 (1996)
27 A. van Oudenaarden, J.A. Theriot: Nat. Cell Biol. **1**, 493 (1999)
28 F. Gerbal, P. Chaikin, Y. Rabin, J. Prost: Biophys. J. **79**, 2259 (2000)
29 D.K. Fygenson, E. Braun, A. Libchaber: Phys. Rev. E **50**, 1579 (1994)
30 F. Gittes, E. Meyhofer, S. Baek, J. Howard: Biophys. J. **70**, 418 (1996)
31 M.E. Janson, M.E. Dood, M. Dogterom: Mol. Biol. Cell **12**, 173a (2001)
32 K. Visscher, S.P. Gross, S.M. Block: IEEE J. Sel. Top. Quantum Electron. **2**, 1066 (1996)
33 C. Tănase, M. Dogterom, B.M. Mulder: in preparation
34 D. Chrétien, S.D. Fuller, E. Karsenti: J. Cell Biol. **129**, 1311 (1995)
35 M.E. Janson, M. Dogterom: Biophys. J. **82**, 509a (2002)